

Kinetics and Thermochemistry of the Reaction $\text{CCl}_3 + \text{NO} + \text{M} \leftrightarrow \text{CCl}_3\text{NO} + \text{M}$

J. Masanet, F. Caralp, A. A. Jemi-Alade, P. D. Lightfoot, and R. Lesclaux*

Laboratoire de Photophysique et de Photochimie Moléculaire, URA 348 CNRS, Université de Bordeaux I, 33405 Talence Cedex, France

M. T. Rayez

Laboratoire de Physicochimie Théorique, URA 503 CNRS, Université de Bordeaux I, 33405 Talence Cedex, France

Received: July 24, 1992; In Final Form: November 9, 1992

The kinetics and equilibrium constant of reaction 1, $\text{CCl}_3 + \text{NO} + \text{M} \leftrightarrow \text{CCl}_3\text{NO} + \text{M}$, were investigated using pulsed-laser photolysis/time-resolved mass spectrometry at low pressure, 0.5–12 Torr, and flash-photolysis/UV absorption spectrometry at high pressure, 110–760 Torr. These pressure ranges cover most of the fall-off region. Fall-off curves were measured at 263, 298, and 373 K and a determination of the rate constant was performed at 465 K, 760 Torr. RRKM calculations were performed for accurate extrapolation to the low and high pressure limits. The rate expressions obtained are, using the formalism of Troe, $k_1(0) = [(1.4 \pm 0.3) \times 10^{-29}](T/298 \text{ K})^{-(5.5 \pm 0.2)} \text{ cm}^6 \text{ molecule}^{-2} \text{ s}^{-1}$ and $k_1(\infty) = [(7.5 \pm 1.5) \times 10^{-12}](T/298 \text{ K})^{-(1.0 \pm 0.3)} \text{ cm}^3 \text{ molecule}^{-1} \text{ s}^{-1}$, with $F_c = 0.66 \exp(-T/600 \text{ K})$. The collisional efficiency factor $\beta_c = (0.43 \pm 0.04)(T/298)^{-(1.0 \pm 0.2)}$ is reasonable, thereby establishing the consistency between kinetic and thermochemical data. The rate expression at 760 Torr is $k_1(760 \text{ Torr}) = [(5.2 \pm 1.0) \times 10^{-12}](T/298)^{-(2.65 \pm 0.2)} \text{ cm}^3 \text{ molecule}^{-1} \text{ s}^{-1}$. The equilibrium constant was measured at 480 and 486 K and the entropy of reaction was calculated using statistical thermodynamics, with the purpose of determining the enthalpy of reaction: $\Delta H^\circ_{298} = -125 \pm 8.5 \text{ kJ mol}^{-1}$. This value, corresponding to the bond dissociation energy $D(\text{CCl}_3\text{--NO})$, is significantly smaller than the corresponding bond dissociation energies in CH_3NO and in CF_3NO : 172 and 167 kJ mol^{-1} , respectively. Ab initio calculations of the above bond dissociation energies have yielded values in good agreement with experimental data.

Introduction

The association reaction of free radicals with NO, forming nitroso compounds, is a well-known reaction which has been extensively used for radical scavenging in various chemical systems. In contrast, the kinetics of these reactions have received only little attention and, in particular, few data are available on their fall-off behavior.

The most extensively studied reactions to date are those of CH_3 ^{1–8} and CF_3 ^{7,9–11} detailed descriptions of the fall-off have been reported for the association reactions of these two species over wide ranges of pressure and temperature.^{8,11} In both cases, the fall-off extends to above 1 atm pressure and the rate constant exhibits a strong negative temperature coefficient, particularly near the low pressure limit. A fairly good agreement between the different experimental studies is observed and theoretical calculations, using the inverse Laplace transformation method for CH_3 ⁸ or RRKM calculations for CF_3 ,¹¹ have accounted for these experimental results in a satisfying manner. Calculations have also accounted correctly for the low-pressure limiting rate constant, the value of which is an order of magnitude higher for CF_3 than for CH_3 . The main reason for this difference is the higher density of states in CF_3NO compared to CH_3NO , due to lower vibrational frequencies, the C–N bond dissociation energies being very close to each other in the two molecules: 167 kJ mol^{-1} for CF_3NO and 172 kJ mol^{-1} for CH_3NO .¹²

Bond dissociation energies are important parameters which influence the low pressure limiting rate constants of association and dissociation reactions. This parameter has been determined accurately for a number of nitroso compounds (CH_3NO , CF_3NO , CCl_2FNO , and CClF_2NO) using spectroscopic methods.¹² However, such methods could not be applied in the case of CCl_3NO

as no structure could be observed in the spectrum.¹² A value of $D(\text{CCl}_3\text{--NO}) = 134 \text{ kJ mol}^{-1}$ was determined by Carmichael et al.,¹³ using the electron impact method. However, this value should be used with caution as, in the same study, the authors determined a value of $D(\text{CF}_3\text{--NO}) = 130 \text{ kJ mol}^{-1}$, which is much too low compared to the accurate spectroscopically determined values.^{12,14} In addition, this low value is not consistent with the kinetic data reported on the dissociation reaction of CF_3NO ¹⁵ and more recently for the combination reaction of CF_3 with NO.¹¹

Very few data on the kinetics of the reaction of CCl_3 with NO are available in the literature.^{16,17} In ref 16, CCl_3 was produced by pulse radiolysis of SF_6 in the presence of CHCl_3 and the reaction with NO was studied at a pressure of 1 atm SF_6 , over the temperature range 298–355 K. Some experiments, carried out at 500 mbar, showed no significant pressure dependence over the range 500–1000 mbar at 298 K. In ref 17, the determination of k_1 was performed with a traditional relative rate technique, using nitrogen as the third body.

In this paper, we report a detailed investigation of the kinetics and thermochemistry of reaction 1:



Two methods were employed for measuring rate constants for reaction 1. At low pressures (1–12 Torr) measurements were performed using pulsed laser photolysis and time-resolved mass spectrometry, by monitoring the rate of formation of CCl_3NO . At high pressures (110–760 Torr) flash photolysis was used for monitoring the removal of CCl_3 by UV absorption spectrometry. Kinetic measurements were performed over the temperature range 263–373 K. The flash photolysis/UV absorption technique was also used for measuring the equilibrium constant of reaction 1, –1 at around 480 K. This measurement allowed a new determination of the C–N bond dissociation energy in CCl_3NO to be made.

* Author to whom correspondence should be addressed.

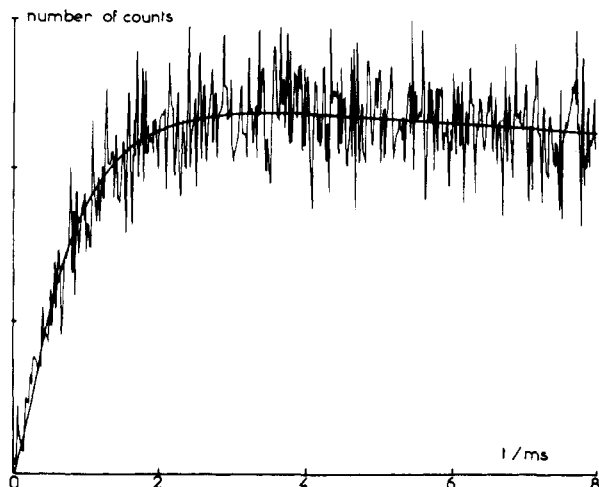


Figure 1. Example of time-resolved mass spectrometric signal of CCl_3NO build up, 1000 runs accumulated: total gas density, 5.2×10^{16} molecules cm^{-3} ; $T = 373$ K; buffer gas, N_2 ; $[\text{NO}] = 1.2 \times 10^{16}$ molecules cm^{-3} ; $[\text{CCl}_3\text{Br}] = 1.0 \times 10^{14}$ molecules cm^{-3} ; number of counts at the maximum, 120. The solid line is the result of numerical simulations obtained by adjusting k_1 .

In addition, RRKM calculations were performed with the principal aim of establishing the consistency of the structural properties of the molecule, the thermochemistry of the reaction, and the experimental kinetic data obtained in the present work. RRKM calculations also allow a critical analysis of the present data when they are compared to those of similar reactions involving other radicals.

Results

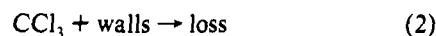
(A) Low-Pressure Measurements Using Mass Spectrometric Detection. Apparatus. The experimental setup has been described previously.¹⁸ The CCl_3 radicals were generated by pulsed laser photolysis of CCl_3Br at 248 nm, using an excimer laser (Lambda Physics EMG 101) and the build up of CCl_3NO was monitored using time-resolved mass spectrometry. The initial CCl_3 concentration has been estimated to be lower than 10^{12} molecules cm^{-3} .¹⁸

The gas mixture was continuously renewed by a controlled flow through the reactor. The concentration of each component was determined by measuring both its flow rate and the total pressure in the reactor. The time-resolved concentration of CCl_3NO was monitored by mass spectrometry (quadrupole BALZERS QMG 511), using molecular beam sampling. The signal was detected at $m^+/e = 112$, corresponding to the fragment ion CCl_2NO^+ (ionization energy, 60 eV). The possibility of any interference in kinetic measurements by a possible direct formation of CCl_2 radicals in the photolysis of CCl_3Br was excluded as discussed in our preceding papers.^{19,20} No signal could be detected at the parent ion mass, in contrast to what was observed in the case of CF_3NO .¹¹ The time-resolved concentration profiles of CCl_3NO were stored in a multiscaler (TRACOR) and transferred to a microcomputer for data processing. Generally, 1000–2500 shots were accumulated for an acceptable signal-to-noise ratio. The buffer gas was nitrogen in all cases. At the lowest pressures (<1 Torr) care was taken to keep a large excess of nitrogen by using very small partial pressures of CCl_3Br (<6 mTorr). Similarly, NO concentrations were always smaller than 1.2×10^{15} molecules cm^{-3} (≈ 300 mTorr).

Products. Nitrogen (99.995%) and NO (99.9%) were provided by l'Air Liquide and used without further purification. CCl_3Br (>99%), supplied by Fluka, was carefully degassed at low temperature.

Results. A typical time-resolved build up of CCl_3NO is shown in Figure 1. The signal was actually recorded over a longer time

than that shown in Figure 1, for an accurate determination of the decay rate of CCl_3NO . This decay was mainly due to transport by the flowing gas mixture, although losses on the walls of the reactor may also have contributed to some extent. The decay, which had typical rates of $10\text{--}20$ s^{-1} , was included in the reaction mechanism and accounted for by a first-order loss process. The simulation of the formation of CCl_3NO was then performed by numerical integration with the following simple reaction mechanism:



Due to the low radical concentrations, the recombination of CCl_3 radicals with themselves or with bromine atoms was neglected. The rate of losses of CCl_3 radicals to the walls was estimated from the intercepts of plots of the pseudo-first-order rates of CCl_3NO production vs $[\text{NO}]$. The intercept varied somewhat from one run to the other and the average value was found to decrease with temperature from around 100 s^{-1} at the lowest temperatures to near zero at 373 K. This is significantly less than the range of pseudo-first-order rate constants typically employed ($400\text{--}2500$ s^{-1}). This average wall loss rate, determined at each temperature, was set equal to k_2 . An error of 100% on k_2 results in a maximum error of about 10% on k_1 at the lowest temperature. The rate constant k_1 was then adjusted in order to fit the experimental signal over a period of approximately 10 ms, by computer simulation of the above mechanism, using a nonlinear least-squares method. The increase of the rate of wall reactions with decreasing temperature can be understood if CCl_3 radicals react with adsorbed species.

The experimental conditions were the following: total gas concentration, $(0.15\text{--}3.5) \times 10^{17}$ molecules cm^{-3} (0.5–12 Torr), buffer gas N_2 ; temperature of measurements, 263, 298, and 373 K; CCl_3Br concentration, $(2\text{--}5) \times 10^{14}$ molecules cm^{-3} ; initial CCl_3 concentration, $\leq 10^{12}$ molecules cm^{-3} ; NO concentration, $(2\text{--}120) \times 10^{14}$ molecules cm^{-3} , corresponding to reaction rates varying from 400 to 2500 s^{-1} ; flow rate, varied by about a factor of 10; laser frequency, 0.4–1.5 Hz. The flow rate and the laser frequency were adjusted so that the gas mixture in the reactor was almost completely renewed between two laser pulses. Measurements at lower temperatures were discarded, due to a poor reproducibility of results. This may have resulted from association reactions of bromine atoms with CCl_3 radicals, becoming significantly fast at low temperature. Such behavior was not observed at the temperatures mentioned above. At 263 K and around 10 Torr, however, similar reasons may explain the values of k_1 , which appear slightly too high compared to the values obtained either at other temperatures or in high pressure measurements using flash photolysis. However, a few experiments performed at this particular temperature, using the photolysis of CCl_4 at 193 nm as a source of CCl_3 and propane as Cl atom scavenger, did not yield values significantly different from those reported below, obtained using CCl_3Br as the precursor.

The pseudo-first-order rates of CCl_3NO formation, corrected for the wall loss of CCl_3 , are plotted against NO concentrations in Figure 2 for a total gas density of $(3.25 \pm 0.25) \times 10^{17}$ molecules cm^{-3} . Linear plots were obtained, suggesting that the experimental conditions and the model used to interpret the kinetics were correct. The slopes of the lines give the bimolecular rate constants k_1 . The large difference in the slopes of the plots in Figure 2 illustrates the fairly strong negative temperature coefficient of k_1 at low pressures.

All the values of k_1 , obtained at different temperatures and different pressures, are listed in Table I and are plotted as fall-off curves in Figure 3 (open symbols). The number of runs corresponding to each value is indicated in the table; the reported

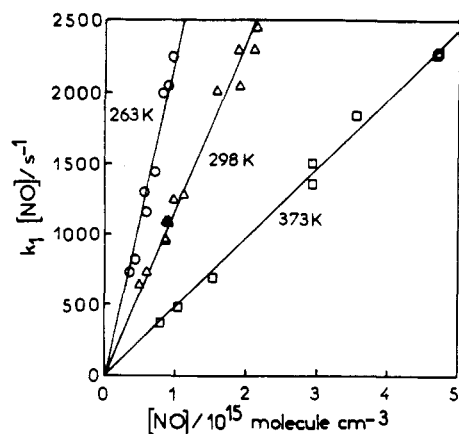


Figure 2. Pseudo-first-order rates of the reaction of CCl_3 with NO plotted as a function of NO concentration: total gas density, $(3.25 \pm 0.25) \times 10^{17}$ molecules cm^{-3} ; buffer gas, N_2 .

TABLE I: Bimolecular Rate Constants, k_1 , Measured by Pulsed-Laser Photolysis/Time-Resolved Mass Spectrometry

temperature, K	total gas density $\times 10^{16}/\text{molecule cm}^{-3}$	no. of runs	$k_1 \times 10^{13}/\text{cm}^3 \text{ molecule}^{-1} \text{ s}^{-1}$
263	3.70	7	4.0 ± 0.2
	7.35	7	7.3 ± 0.4
	14.7	9	15.0 ± 1.0
	22.1	4	17.6 ± 1.0
	29.4	8	22.4 ± 2.0
	36.8	6	28.2 ± 2.0
298	44.2	6	31.0 ± 1.9
	1.62	2	1.6 ± 0.3
	3.25	10	2.4 ± 0.1
	6.5	7	4.2 ± 0.3
	13.0	11	6.1 ± 0.5
	16.2	4	7.2 ± 0.3
	19.5	5	8.1 ± 0.4
	26.0	26	10.3 ± 0.3
32.5	15	11.6 ± 0.4	
373	39.0	14	13.4 ± 1.0
	3.90	7	1.0 ± 0.1
	5.20	7	1.2 ± 0.1
	10.4	8	2.1 ± 0.1
	13.0	5	2.4 ± 0.2
	15.6	5	2.9 ± 0.1
	19.5	5	3.5 ± 0.5
	20.8	7	3.6 ± 0.3
26.0	13	4.2 ± 0.2	
31.2	8	4.9 ± 0.4	

values of k_1 were obtained using a least-squares treatment of the data. Figure 3 shows that the data obtained in the present low-pressure range are close to the third-order limit. The closed symbols in the figure are the data obtained at high pressure, as reported in the next section.

(B) High-Pressure Measurements Using Flash Photolysis and UV Absorption Detection. Apparatus. The flash photolysis system used here has been described in detail elsewhere.²¹ Briefly, a cylindrical quartz reaction cell, 70 cm in length and 4.5 cm in diameter was situated in an electrically heated oven. Temperature measurements were made using three K-type thermocouples placed along the outside of the cell; the temperature of the cell was stable to $\pm 1\%$. Photolysis was provided by an argon flash lamp located parallel to the reaction cell within the oven. The quartz flash lamp was surrounded by a concentric Pyrex tube to filter out light at $\lambda < 280$ nm. A deuterium lamp was used as the analysis light source, the beam passing twice through the cell, resulting in an effective path length of 140 cm, and impinging on a monochromator-photomultiplier assembly unit. Signals were stored in a digital storage oscilloscope and transferred to a microcomputer for averaging, followed by analysis using numerical integration/nonlinear least squares. Typically, 10–30 shots were averaged to obtain adequate signal-to-noise ratios.

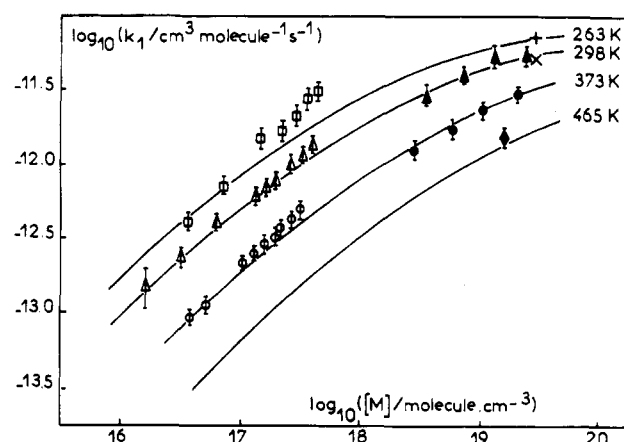
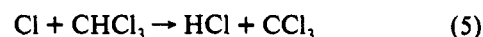


Figure 3. Pressure dependence of the bimolecular rate constant k_1 : open symbols, low-pressure results obtained by laser photolysis/time-resolved mass spectrometry; closed symbols, high-pressure results obtained by flash-photolysis/UV absorption detection; (+) extrapolated from other temperature measurements using the expression of k_1 obtained at 1 atm pressure (see text); (X) value of k_1 from ref 37. Solid lines are RRKM fall-off curves fitted to experimental data.

Trichloromethyl radicals were generated by flashing molecular chlorine in the presence of chloroform



$$k_5 = (1.45 \times 10^{-11}) \exp(-1380/T) \text{ cm}^3 \text{ molecule}^{-1} \text{ s}^{-1,22}$$

The concentration of chloroform was sufficient to ensure that reaction 5 was complete within the flash duration (around 5 μs) and to prevent Cl atoms from reacting with CCl_3 ²³ and with NO .²⁴

The UV absorption spectrum of CCl_3 has been reported in a previous publication.²³ CCl_3 has an absorption band peaking at 211 nm with a fairly high absorption cross section: $\sigma = 1.45 \times 10^{-17} \text{ cm}^2 \text{ molecule}^{-1}$. Most kinetic measurements were performed at 220 nm where the signal-to-noise ratio was maximum. At this wavelength, the absorption cross section of CCl_3 is $9.9 \times 10^{-18} \text{ cm}^2 \text{ molecule}^{-1}$,²³ and that of CCl_3NO is $1.2 \times 10^{-18} \text{ cm}^2 \text{ molecule}^{-1}$ at room temperature.²⁵ The large difference between these values allowed the conversion of CCl_3 into CCl_3NO to be easily monitored by UV absorption.

In order to rigorously exclude traces of oxygen from the system, experimental $\text{Cl}_2/\text{CHCl}_3/\text{N}_2$ mixtures were passed through a small cell which was irradiated with light from a medium-pressure mercury lamp. In this way, a very small fraction ($< 1\%$) of the molecular chlorine was photodissociated and small quantities of CCl_3 radicals were formed. These radicals reacted with any traces of molecular oxygen present to form CCl_2O ²² in very low yield ($< 1 \times 10^{14}$ molecules cm^{-3}), which did not interfere with the production or the subsequent reaction of the CCl_3 radicals. The nitric oxide reactant was added into the flowing gas mixture after this treatment and so was unaffected by it. The final $\text{Cl}_2/\text{CHCl}_3/\text{NO}/\text{N}_2$ mixture was continuously flowed through the reactor with a residence time of around 30 s, so that it was renewed after each flash. Concentrations were determined for each component from its flow rate and from the total pressure.

Products. Nitrogen (99.995%, l'Air Liquide) and chlorine (5% in nitrogen, l'Air Liquide), were used directly from the cylinder. Chloroform (Aldrich, spectroscopic grade) contained 0.5–1% of ethanol for stabilization, which was removed either by distillation or by storage over molecular sieve, under a nitrogen atmosphere.

Results. Owing to the relatively low sensitivity of UV absorption detection compared to the mass spectrometry technique, fairly high radical concentrations ($(4-10) \times 10^{13}$ molecules cm^{-3}) had to be used in these experiments to obtain good signal-to-noise ratios. Consequently, the following reaction mechanism, including

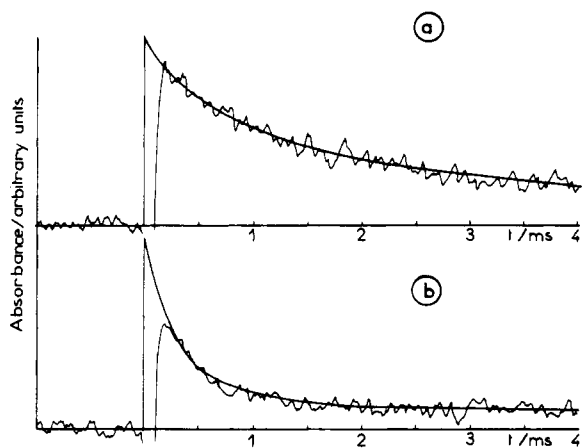
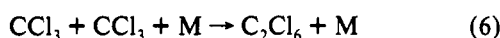
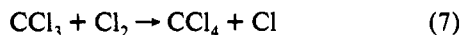


Figure 4. CCl_3 decay traces obtained by flash photolysis/UV absorption: (a) in the absence of NO; (b) in the presence of 4.95×10^{-14} molecule cm^{-3} of NO. The maximum absorbance at $t = 0$ is 0.083.

radical—radical reactions, was used to simulate the experimental traces:



However, unlike the low-pressure experiments, wall losses and pump-out were completely negligible at the higher pressure of these experiments and were not included in the analysis. Similarly, the potential secondary reaction of CCl_3 with Cl_2



is too slow under the present experimental conditions to be important;²⁶ the chlorine atoms generated in reaction 7 would, in any case, rapidly regenerate CCl_3 radicals via reaction 5. It should be emphasized that only reactions 1 and 6 had an important contribution to the decay of CCl_3 ; the contribution of reaction 6 was significant, particularly at low NO concentrations, as fairly high initial concentrations of radicals had to be used. The kinetics of reaction 6 has been investigated in detail in this laboratory,²³ giving $k_6 = [3.3 \times 10^{-12}](T/298)^{-1.0} \text{ cm}^3 \text{ molecule}^{-1} \text{ s}^{-1}$, independent of pressure over the temperature range of the present study. Simulations of the decay traces show that an uncertainty of 20% in k_6 results in an error smaller than 2% in k_1 .

The experimental conditions were as follows: total pressure, 110–760 Torr N_2 ; temperature, 298, 373, and 465 K (measurements at lower temperature were not possible with this apparatus); concentration of molecular chlorine, $(1.5\text{--}4.6) \times 10^{16}$ molecules cm^{-3} ; concentration of chloroform, $(0.9\text{--}3.6) \times 10^{17}$ molecules cm^{-3} ; initial concentration of CCl_3 , $(8\text{--}15) \times 10^{13}$ molecules cm^{-3} ; concentration of NO, $(1.8\text{--}12.9) \times 10^{14}$ molecules cm^{-3} . Experiments were carried out at four pressures, 110, 220, 400, and 760 Torr at both 298 and 373 K, and at 760 Torr at 465 K. At each temperature and pressure, reaction 6 was studied before and after reaction 1. The optimized parameters were the initial radical concentration and k_6 ; for experiments with added NO, the optimized parameters were k_1 and the absorption cross section of CCl_3NO , the initial concentration of CCl_3 being the same as in the experiments performed in the absence of NO, where it can be determined more accurately due to the slower initial decay.

Typical optical density–time traces are given in Figure 4 for two different experimental conditions. Figure 4a represents the decay of the CCl_3 radical in the absence of NO, according to second-order kinetics due to reaction 6 alone. The decay trace shown in Figure 4b is obtained in the presence of a concentration of NO suitable for the measurement of k_1 . The figure shows that the experimental trace could be well reproduced by computer simulation (full lines) of the above reaction mechanism.

The results are given in Table II. No systematic dependence of the kinetics or product absorption cross sections on Cl_2

concentration, flash lamp energy, or NO concentration was observed, given the concentration ranges and conditions stated above. No pressure dependence was found for reaction 6, which is in agreement with our previous study.²³ The optimized absorption cross sections for CCl_3NO , even under conditions where a significant fraction of the CCl_3 radicals react via reaction 6, are in good agreement with the room temperature measurement of Allston et al.,²⁵ giving us further confidence in the results. The closed symbols on the fall-off curves in Figure 3 represent the data obtained in these high-pressure measurements. It can be seen that both the rate constants and their temperature dependence are consistent with those obtained at low pressure, using a very different technique. The negative temperature coefficient is still fairly high at 760 Torr, where the rate constant is only around 30% below the high pressure limit at room temperature. This results, when fitting the whole data, in a negative temperature coefficient for the high pressure limit, as shown in following sections.

The rate expression of k_1 measured at 760 Torr is

$$k_1(760 \text{ Torr}) = [(5.2 \pm 1.0) \times 10^{-12}] \times (T/298)^{-(2.65 \pm 0.2)} \text{ cm}^3 \text{ molecule}^{-1} \text{ s}^{-1}$$

(C) Equilibrium Constant and Enthalpy of Reaction 1. It was emphasized above that, until now, no reliable value of the bond dissociation energy $D(\text{CCl}_3\text{--NO})$ has been available. Since this is an important parameter in calculations of rate constants using unimolecular theories, particularly in the low pressure range of the fall-off, it was measured as part of the present study. The equilibrium constant of reaction 1 was measured at around 480 K and $D(\text{CCl}_3\text{--NO})$ calculated using third law methods; the entropy of reaction 1 was calculated using statistical thermodynamics.

Experimental Determination of the Equilibrium Constant. The equilibrium constant was measured using the flash photolysis/UV detection equipment under experimental conditions similar to those described in the preceding section. With the temperature above 470 K, the decay of CCl_3 became more complex than that observed at lower temperatures and could no longer be simulated using the simple reaction mechanism above. The residual absorption due to CCl_3NO decayed slowly on a timescale which was long compared to that of its formation; this could be interpreted by considering that reaction -1 becomes important at these temperatures, resulting in a pseudo-steady-state concentration of CCl_3 radicals which were slowly removed via reaction 6.

The equilibration kinetics of reactions 1, -1 were studied at 760 Torr total pressure and at two temperatures: 480 and 486 K. The temperature 480 K was the lowest temperature at which equilibrium was observed. Equilibrium was manifested by a slow fall-off of the CCl_3NO absorption observed at 220 nm, as is shown in Figure 5b. At a temperature below that at which equilibrium was observed, CCl_3NO appears stable: Figure 5a. Note that the timescale for the traces in Figure 5 is very much longer than that for the traces in Figure 4. Values of $K_c = (k_1/k_{-1})$ were obtained by simultaneously fitting, as described previously,²¹ pairs of decay traces of experiments carried out over timescales of 5 and 51 ms. These timescales were chosen to best allow observation of the approach to and position of the pseudoequilibrium; experiments on the much longer timescales shown in Figure 5b demonstrate the pseudoequilibrium very clearly but provide very little kinetic information. This procedure enabled both k_1 and k_{-1} to be extracted. However, the individual values of k_1 and k_{-1} obtained by this method should be treated with caution since they are somewhat mutually dependent; only their ratio is significant. Simulations of pairs of decay traces were also performed using values of k_1 extrapolated from lower temperature experiments and then optimizing k_{-1} to give the best fit. For both of these methods, the initial concentration of CCl_3 was also optimized.

TABLE II: Bimolecular Rate Constants, k_1 , Measured by Flash-Photolysis/UV Absorption Spectrometry at 220 nm

T/K	total gas density $\times 10^{-18}/\text{molecule cm}^{-3}$	$k_b \times 10^{12}/\text{cm}^3 \text{ molecule}^{-1} \text{ s}^{-1}$	$k_1 \times 10^{12}/\text{cm}^3 \text{ molecule}^{-1} \text{ s}^{-1}$	$\sigma(\text{CCl}_3\text{NO}) \times 10^{18}/\text{cm}^2 \text{ molecule}^{-1}$
298	3.6	3.13 ± 0.23	3.04 ± 0.35	1.42 ± 0.11
	7.2	3.00 ± 0.17	4.12 ± 0.25	1.27 ± 0.08
	13.0	3.13 ± 0.09	5.41 ± 0.75	1.40 ± 0.34
	24.7	3.28 ± 0.14	5.26 ± 0.76	1.36 ± 0.21
373	2.85	2.28 ± 0.13	1.30 ± 0.14	1.29 ± 0.15
	5.7	2.41 ± 0.12	1.82 ± 0.18	1.75 ± 0.17
	10.4	2.45 ± 0.10	2.42 ± 0.17	1.47 ± 0.21
	19.7	2.21 ± 0.17	2.89 ± 0.16	1.44 ± 0.14
465	15.8	1.83 ± 0.12	1.62 ± 0.12	2.07 ± 0.25

TABLE III: Equilibrium Constant Measurements

T/K	three-parameter fits			two-parameter fits			
	$10^{-14}[\text{NO}]^a$	$10^{12}k_1^b$	k_{-1}^c	$10^{-4}K_p^d$	$10^{12}k_1^b$	k_{-1}^c	$10^{-4}K_p^d$
480	10.6	1.22	187	10.0	1.47	160	14.0
	5.30	0.99	199	7.6	1.47	258	8.7
	2.74	1.04	195	8.1	1.47	265	8.5
486	10.4	1.01	205	7.4	1.42	177	12.1
	7.77	0.86	231	5.7	1.42	296	7.3
	5.18	0.84	212	6.1	1.42	312	6.9

^a Units of molecule cm^{-3} . ^b Units of $\text{cm}^3 \text{ molecule}^{-1} \text{ s}^{-1}$. ^c Units of s^{-1} . ^d Units of atm^{-1} .

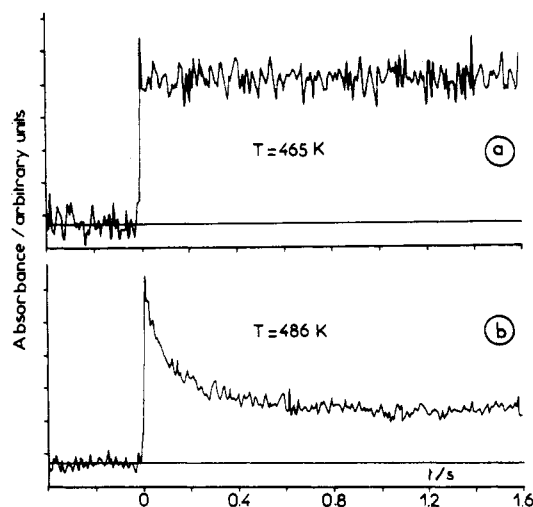


Figure 5. CCl_3NO absorption traces ($\lambda = 220 \text{ nm}$) obtained below (a) and at (b) the temperature at which equilibrium of reaction 1 is observed. The maximum absorbance on the vertical scale is 0.028. $[\text{NO}] = 1.0 \times 10^{15} \text{ molecule cm}^{-3}$, atmospheric pressure, buffer gas N_2 .

The results of these methods are shown in Table III. At each of the two temperatures the values of K_p obtained by the two methods were averaged, giving $K_p = (95 \pm 24) \times 10^3 \text{ atm}^{-1}$ at 480 K and $K_p = (76 \pm 23) \times 10^3 \text{ atm}^{-1}$ at 486 K.

At higher temperatures, the effect of the reverse reaction -1 became progressively more important, but no quantitative information could be obtained owing to experimental difficulties; the optical density traces returned below the preflash baseline. After much effort, it was concluded that this effect was due to the presence of significant concentrations of CCl_3NO and possibly NOCl in the reactor, produced by a thermal reaction involving the dissociation of a small fraction of molecular chlorine, possibly on the walls of the reactor. Some thermal decomposition of molecular chlorine has been observed in our apparatus at high temperatures on previous occasions^{21,27} but usually poses no problem, as the chlorine atoms produced generally react to form the usual products of the reaction under study. Both CCl_3NO and NOCl ($\sigma/\text{cm}^2 \text{ molecule}^{-1} = 8.96 \times 10^{-18}$ at 220 nm ²⁴) absorb strongly at the monitoring wavelength and a shift in the postflash baseline could be attributed to their removal, either by direct photolysis or by reaction with the atoms.

As discussed below, although equilibrium constants could only be measured over a very narrow temperature range and the

TABLE IV: Structural Parameters Used in Calculations

CCl_3NO	CCl_3	NO
Vibrational Frequencies/ cm^{-1}		
1619 ^a	898 ^c	1904
942 ^a	898 ^c	
880 ^a	487 ^c	
812 ^a	266 ^c	
696 ^a	266 ^c	
637 ^a	umbrella mode ^f	
431 ^a		
305 ^a		
272 ^a		
221 ^b		
188 ^b		
50 ^b		
Moments of Inertia/ 10^{-38} g cm^2		
4.69 ^b	2.69 ^b	0.164 ^b
5.05 ^b	2.59 ^b	
5.41 ^b	5.17 ^b	
Lennard-Jones Parameters		
$\sigma(\text{CCl}_3\text{NO}) = 5.95 \text{ \AA}^c$	$\sigma(\text{N}_2) = 3.63 \text{ \AA}$	
$\epsilon/k(\text{CCl}_3\text{NO}) = 322.7 \text{ K}^c$	$\epsilon/k(\text{N}_2) = 91.5 \text{ K}$	

^a From ref 28. ^b Calculated using the MNDO semiempirical method. ^c From ref 31. ^d From JANAF Tables (ref 45). ^e Values for CCl_4 . ^f See text and ref 31.

uncertainty in them is rather large, they allow $D(\text{CCl}_3\text{-NO})$ to be determined to a much greater precision than has been previously possible.

Thermochemistry of Reaction 1. As the equilibrium constant was measured over a very narrow temperature range, only the third law method can yield a reliable determination of the enthalpy of reaction 1, by calculating the intercept, $\Delta S^\circ/R$, of the van't Hoff plot. The entropy change of the reaction was calculated by using statistical thermodynamics, with the structural parameters given in Table IV. The nine highest fundamental vibrational frequencies of CCl_3NO were determined by Ernsting and Pfab²⁸ from infrared spectra. The remaining three lowest frequencies and the three moments of inertia were calculated for the present work using the semiempirical MNDO method.²⁹ Reasonably good agreement was observed between the nine experimental and calculated frequencies.

The molecular parameters adopted for the CCl_3 radical (Table IV) were those determined by Hudgens et al.^{30,31} The vibrational frequencies were obtained either from spectroscopic data or from scaled ab initio calculations. The umbrella mode is highly anharmonic, due to the presence of two shallow wells on the potential energy surface.³¹ Thus, the corresponding partition function and entropy had to be calculated using an explicit summation over the first 48 energy levels of the manifold given in ref 31. In the RRKM calculations (vide infra), this umbrella mode is represented by a harmonic vibrator whose vibrational frequency (different at each temperature) corresponds to the same partition function as that derived from the exact calculation. As the Lennard-Jones parameters of CCl_3NO are unknown, those of CCl_4 were used instead.

Since thermochemical data are generally given at room temperature, the calculations were performed at 298 K. The

following values of entropies were obtained: $S^\circ_{298} = (349.5 \pm 6.3) \text{ J mol}^{-1} \text{ K}^{-1}$ for CCl_3NO (uncertainties are essentially due to the three lowest calculated vibrational frequencies), $S^\circ_{298} = (301.3 \pm 2.1) \text{ J mol}^{-1} \text{ K}^{-1}$ for CCl_3 ³¹ and $\Delta S^\circ_{298} = -(164 \pm 6.6) \text{ J mol}^{-1} \text{ K}^{-1}$ for reaction 1.

The modified van't Hoff expression, which takes into account the fact that K_c and ΔS° were determined at different temperatures, was used for the determination of the reaction enthalpy at 298 K:

$$\ln[K_p(T)] - 1/R \int_{298}^T (\Delta C_p/T) dT + 1/RT \int_{298}^T (\Delta C_p) dT = \Delta S^\circ_{298}/R - \Delta H^\circ_{298}/RT$$

In fact, the difference between the two integrals correcting $\ln[K_p(T)]$ in the above equation was negligible for the small temperature difference considered in the present case.

The calculated value of the entropy of reaction and the values of the equilibrium constant at 480–486 K yield for the enthalpy of reaction 1 and consequently for the bond dissociation energy $D(\text{CCl}_3\text{--NO})$ $\Delta H^\circ_{298} = -(125 \pm 8.5) \text{ kJ mol}^{-1}$. This results in an enthalpy of formation $\Delta H^\circ_f = (37.7 \pm 11.0) \text{ kJ mol}^{-1}$ for CCl_3NO at 298 K, using $\Delta H^\circ_f(\text{CCl}_3) = (71.1 \pm 2.5) \text{ kJ mol}^{-1}$ ³¹ and $\Delta H^\circ_f(\text{NO}) = (91.3 \pm 0.2) \text{ kJ mol}^{-1}$.³² The enthalpy change of reaction 1 at 0 K was calculated using the following expression for the equilibrium constant

$$K_c = [Q(\text{CCl}_3\text{NO})/Q(\text{CCl}_3)Q(\text{NO})] \exp(-\Delta H^\circ_0/RT) \quad (\text{I})$$

where the Q 's are the total partition functions of the species involved. Calculations performed for the two experimental values of K_c give $\Delta H^\circ_0 = -(120 \pm 8.4) \text{ kJ mol}^{-1}$. This parameter was taken as the critical energy E_0 in RRKM calculations.

Equation I was used to generate a van't Hoff-like expression for K_c , valid over the temperature range 300–700 K:

$$K_c = (3.7 \pm 2.0) \times 10^{-28} \times \exp[(14625 \pm 1020)/T] \text{ cm}^3 \text{ molecule}^{-1}$$

This expression gives values of K_c with an uncertainty of about a factor 2 around 450–500 K.

(D) RRKM Calculations. There are several interesting aspects in performing RRKM calculations on reaction 1 to complement the experimental data. In the first place, it helps to extrapolate the kinetic results to pressure and temperature ranges that cannot be investigated experimentally. Secondly, it allows us to verify the consistency between the kinetic data obtained in this work and the thermochemical and structural properties of the species involved in reaction 1. In addition, the RRKM model can be the base for a general model that can be applied to a homogeneous series of reactions such as those of CCl_3 , CCl_2F , CClF_2 , and CF_3 with NO. It also represents a further test for unimolecular theories.

RRKM calculations were performed for the unimolecular dissociation of CCl_3NO in a similar way to those performed for CF_3NO ,¹¹ using the procedure reported in previous papers.^{11,33} Rate constants for the association reaction were obtained by using the equilibrium constant determined in the preceding section. All parameters necessary for the calculations, i.e. vibrational frequencies, moments of inertia, and Lennard-Jones parameters, are listed in Table IV. The experimental temperature dependence of k_1 shows that the reaction does not involve any potential barrier on the reaction coordinate and consequently the value of ΔH°_0 determined above was taken as the critical energy E_0 in the calculations.

The modified Gorin model³⁴ was chosen for the transition state: the seven vibrational frequencies of the "conserved" degrees of freedom were taken as equal to those of the fragments CCl_3 and NO; the C–N stretch was taken as the reaction coordinate; the deformation and torsional modes were treated as two two-

dimensional restricted rotors, with an adjustable hindrance parameter, η , taking into account the restriction of the rotors.³⁴ Since the Gorin model is unable to account for the temperature dependence of k_1 at the high-pressure limit, the hindrance parameter η was adjusted at each temperature to reproduce the experimental results. At low pressures, the collisional efficiency factor β_c had to be introduced since the strong collision approximation was used in the calculations; β_c was also found temperature dependent.

Results of Calculations. Calculations were carried out at four temperatures, 263, 298, 373 and 465 K, corresponding to the experimental measurements of k_1 . The expression derived from calculations for the third-order strong collision rate constant is

$$k_1^{sc}(0) = (4.0 \times 10^{-29})(T/298)^{-4.5} \text{ cm}^6 \text{ molecule}^{-2} \text{ s}^{-1}$$

This expression shows the fairly strong negative temperature coefficient calculated for k_1 at low pressure.

Both the parameters β_c and η were adjusted at each temperature to obtain the best agreement between the calculated and experimental data. The experimental third-order rate constant $k_1(0) = \beta_c k_1^{sc}(0)$ exhibited a stronger negative temperature coefficient than the calculated strong collision expression, so that a negative temperature dependence had to be assigned to the coefficient β_c .

$$\beta_c = (0.43 \pm 0.04)(T/298)^{(-1.0 \pm 0.2)}$$

Finally, calculations using the above treatment resulted in the solid lines, shown in Figure 3. This set of fall-off curves is thought to be the best synthetic representation of the whole experimental data obtained in this work.

These data can be conveniently reported by using the analytical expression introduced by Troe.³⁵ By fitting this expression to the results of RRKM calculations, the expressions giving $k_1(0)$, $k_1(\infty)$, and the broadening factor F_c as a function of temperature were derived:

$$k_1(0) = [(1.4 \pm 0.3) \times 10^{-29}] \times (T/298)^{(-5.5 \pm 0.2)} \text{ cm}^6 \text{ molecule}^{-2} \text{ s}^{-1}$$

$$k_1(\infty) = [(7.5 \pm 1.5) \times 10^{-12}] \times (T/298)^{(-1.0 \pm 0.3)} \text{ cm}^3 \text{ molecule}^{-1} \text{ s}^{-1}$$

$$F_c = 0.66 \exp(-T/600)$$

The expression of Troe with the above parameters yields a fairly good representation of the RRKM curves and, therefore, of the experimental data. The simple expression for F_c commonly used, $F_c = \exp(-T/C)$, where C is a constant, was not used in the present case, as it did not yield a good representation of the data over the whole temperature range. The agreement was particularly poor at 465 K and the three lowest temperatures could be represented correctly with $F_c = \exp(-T/325)$. The proposed two-parameters expression given above is a simplification of the two-exponential/four-parameter expression proposed by Wagner and Wardlaw;³⁶ the latter is intended for much wider temperature range than the present one.

Discussion

Accuracy of Kinetic Results and Comparison with Other Data. The experimental results obtained in this work, concerning the kinetics of reaction 1, provide a comprehensive description of the fall-off behavior of reaction 1, between about 1 Torr and 1 atm pressure. These original data, obtained in both the low-pressure and the high-pressure ranges of the fall-off, allow reliable extrapolations to the low- and high-pressure limits of the bimolecular rate constant k_1 .

In low-pressure experiments, the dispersion of individual determinations of k_1 (Table I) is typically 10% (1σ) and it can

be evaluated that the extrapolation to the low-pressure limit should result in an error smaller than 20% for $k_1(0)$. Any systematic error might arise from losses of CCl_3 radicals on the walls. However, these losses have been taken into account and we have shown that they might result in a maximum error of about 10% on k_1 . It is worth noting that the experimental results and those of RRKM calculations are quite consistent, except around 6–10 Torr at 263 K, where the measured values of k_1 seem slightly too high compared to the whole set of data. The value of 0.43 obtained for $\beta_c(\text{N}_2)$ at room temperature is reasonable, even though it lies at the upper limit of the values usually observed for this parameter. It should be emphasized, however, that the calculated strong collisions rate constant $k_1^{\text{sc}}(0)$ is highly dependent on the threshold energy E_0 , which has been determined, as discussed below, with a fairly large uncertainty. The value of β_c is therefore influenced by this uncertainty. For example, if E_0 was higher by 8 kJ mol⁻¹, i.e. within the uncertainties, β_c would be reduced to 0.25, which is an average value for this parameter.

In the high-pressure experiments, using flash photolysis/UV absorption, the error in individual values of k_1 is also around 10% (1σ). In this case, the self-recombination of CCl_3 radicals had to be taken into account but the chemical system remained simple and was easily accounted for. Therefore, no particular systematic error arising from uncontrolled chemical reactions is expected in these measurements. It should be emphasized that both the low and the high pressure measurements, performed with two very different techniques, are in fairly good agreement for both the rate constant and the temperature dependence (except again for the few values at 263 K and at 6–10 Torr). This consistency between the two sets of experiments, illustrated in Figure 3, gives confidence in our results.

The values of k_1 at 760 Torr are close to the high-pressure limit, more than half the values of $k(\infty)$. This proximity allows a reliable extrapolation to the high pressure limit and results in a limited error on the values of $k_1(\infty)$, it is estimated to be about 25%. However, the bimolecular rate constant $k_1(P, T)$ calculated by using the parameters of Troe's expression, are determined with a better accuracy, around 15%, over the range of pressures (≈ 1 –760 Torr) and temperatures (263–373 K) of the present measurements.

As far as we know, no direct measurements of k_1 have been reported in the literature. Recently, however, k_1 has been measured at high pressure by pulse radiolysis,³⁷ $k_1 = (5.2 \pm 0.9) \times 10^{-12}$ cm³ molecule⁻¹ s⁻¹ at 298 K and 760 Torr, in very good agreement with our data (Figure 3).

We have recently reported the kinetic parameters for the equivalent reaction of the CF_3 radical. At the low-pressure limit, the reaction is significantly faster since $k(0) = 3.2 \times 10^{-29}$ cm⁶ molecule⁻² s⁻¹ at 298 K instead of 1.4×10^{-29} cm⁶ molecule⁻² s⁻¹ for CCl_3 . Taking only into account the structural parameters, particularly the vibrational frequencies which are much lower in CCl_3NO than in CF_3NO , a faster reaction would have been expected for CCl_3 . Thus, the lower rate constant obtained experimentally for CCl_3 can only be explained by a weaker C–N bond dissociation energy in CCl_3NO than in CF_3NO , resulting in a lower density of states. This has been confirmed in this work both by the measurement of the enthalpy of reaction and by the consistency obtained between experimental and calculated kinetic data, using the low value of the C–N bond dissociation energy reported in this work.

At the high pressure limit, the value of $k(\infty)$ is also significantly smaller for CCl_3 than for CF_3 ^{7,11} and CH_3 :^{6,7} 7.5×10^{-12} instead of 2.0 and 1.5×10^{-11} cm³ molecule⁻¹ s⁻¹, respectively. A similar difference was also observed for the reactions of CCl_3 and CF_3 with O_2 .²⁰ According to the modified Gorin model that we have used for the transition state, this can be understood by assuming a larger hindrance in the restricted rotors in the transition state than in other cases, due to the larger size of the CCl_3 moiety.

TABLE V: Experimental and Calculated C–N Bond Dissociation Energies (kJ mol⁻¹)

	experimental	calculated
CCl_3NO	120	118
CFCl_2NO	171.5 ^a	147
CF_2ClNO	163.9 ^a	159
CF_3NO	167.3 ^a	168
CH_3NO	172.3 ^a	166

^a From ref 12, other values from this work.

However, other explanations can be found; for example, the shape of the potential energy curve near the transition state can be influenced by the depth of the potential well or by polar effects.

Thermochemistry of Reaction 1. This work represents the first determination of the bond dissociation energy of CCl_3NO : 125 ± 8.5 kJ mol⁻¹ at 298 K. The uncertainty is essentially due to the equilibrium constant measurements of reaction 1, which were restricted to a very narrow temperature range. As a result, the reaction entropy had to be determined by a statistical thermodynamics calculation. It must be pointed out that this value of the bond dissociation energy is consistent with the present kinetic measurements, particularly in the low pressure range, even though the values of β_c appear a little higher than the average values of this parameter, as discussed above.

In addition, we have used the GAUSSIAN88 program³⁸ to perform ab initio calculations of ΔH°_0 for comparison with the experimental result. Fully optimized geometries and zero-point energy corrections for CCl_3 , NO, and CCl_3NO were calculated at the Hartree–Fock level (UHF for radicals), using the split valence 6-31G* basis set with polarization functions. The geometries were then used for computation of electron correlation with fourth-order Moller–Plesset perturbation theory,³⁹ in the space of single, double, and quadrupole excitations (MP4SDTQ). This level of calculations is denoted by Pople as (MP4SDTQ/6-31G**/HF/6-31G). Taking into account the zero-point level corrections, calculations have yielded $\Delta H^\circ_0 = -118$ kJ mol⁻¹, in very good agreement with the experimental value, -120 ± 8.5 kJ mol⁻¹. Calculations were also performed for the reactions of CH_3 , CF_3 , CF_2Cl , and CFCl_2 with NO. The results are reported in Table V.

The value found experimentally in this work for $D(\text{CCl}_3\text{–NO})$ is 44–52 kJ mol⁻¹ lower than the corresponding values found for other CX_3NO species, which were determined accurately using spectroscopic methods,¹² as shown in Table V. It is seen that this is corroborated by the above ab initio calculations in the cases of CCl_3NO , CF_2ClNO , CF_3NO , and CH_3NO . In the case of CFCl_2NO , however, the calculated C–N bond dissociation energies is significantly smaller than the experimental one (Table V). This discrepancy is not understood at the present time.

The weakening of $D(\text{CCl}_3\text{–R})$, compared to $D(\text{CF}_3\text{–R})$, seems to be the general behavior, as it has been observed previously for $\text{R} = \text{H}$,⁴⁰ Br ,⁴⁰ CF_3 ,⁴⁰ CCl_3 ,³² and O_2 .²² A similar decrease in the C–R bond dissociation energy has also been observed for CCl_3R compounds compared to the CH_3R equivalents;^{31,41,42} for example, it is also around 50 kJ mol⁻¹ for $\text{R} = \text{O}_2$.⁴²

Results of RRKM Calculations. By comparison of the RRKM calculated strong collision rate constant $k_1^{\text{sc}}(0)$ with the experimental value of k_1 , the value of 0.43 was determined for β_c at 298 K. Introducing this value in the expression

$$\beta_c / (1 - \beta_c^{1/2}) = -(\Delta E) / F_E k T$$

gives $(\Delta E) = 310$ cm⁻¹ (the average energy transferred per collision) and a temperature dependence of $T^{-0.7}$ for β_c . In the above expression, F_E is the coefficient which accounts for the energy dependence of the density of states in CCl_3NO . The experimental temperature dependence of $\beta_c (T^{-1})$ is in fairly good agreement with the above calculated value.

A large negative temperature coefficient had also to be assigned to β_c for the reactions of CF_3 and CCl_3 with O_2 ²⁰ ($\approx T^{-2}$), while

it was negligible ($T^{-0.2}$) for the reaction of CF_3 with NO .¹¹ For this latter reaction, however, it was concluded that the negative temperature coefficient should be significantly higher to obtain a better consistency between our results and those obtained by Glänzer et al.¹⁵ at high temperatures. A fairly large temperature dependence of the deactivation efficiency by collisions seems therefore to be a general characteristic of this type of association reactions of halogenated methyl radicals.

The RRKM calculations performed in this work, with a transition state obtained from the modified Gorin model, were carried out with four adjustable parameters: β_c , η , and their respective temperature dependences. Thus, the calculations were used to fit the experimental data, allowing fall-off curves to be generated at all temperatures and $k(0)$ and $k(\infty)$ to be determined from reliable extrapolations of the data. In this way, the fall-off curves ensure a good representation of all our experimental data obtained under various conditions.

A new variational RRKM method has recently been developed by Forst⁴³ and applied with success to several systems.⁴⁴ In this method, the variational transition state is determined by using a switching function, characterized by a parameter "c", allowing an interpolation between the partition functions of products and those of reactants. In this case, the parameter β_c is used in the same way as in the nonvariational method and the parameter "c" is adjusted at a single temperature, instead of adjusting the parameter η at each temperature. The variational method therefore provides a prediction of the temperature dependence of $k(\infty)$. Calculations with this technique yield very similar fall-off curves to those reported above with a temperature dependence of $k(\infty)$ equal to $T^{-0.7}$. This is in good agreement with the experimental results.

This variational procedure is particularly interesting when it is applied to a homologous series of reactions involving similar species. This generally results in a simple correlation between the parameters that describe the potential energy curve along the reaction coordinate and the switching function parameter "c".⁴⁴ In this sense, we can expect that this type of correlation will prove to have predictive power. This method will be applied in a subsequent work to the series of association reactions of CF_3 , CF_2Cl , CFCl_2 , and CCl_3 radicals with NO . Experiments are in progress for CF_2Cl and CFCl_2 for completion of the experimental data concerning this series.

Acknowledgment. The authors wish to thank Dr. W. Forst for helpful discussions about RRKM calculations.

References and Notes

- (1) Allen, E. R.; Bagley, K. W. *Ber. Bunsen-Ges. Phys. Chem.* **1968**, *72*, 277.
- (2) Heicklen, J.; Cohen, N. *Adv. Photochem.* **1968**, *5*, 275.
- (3) Basco, N.; James, D. G. L.; Stuart, R. S. *Int. J. Chem. Kinet.* **1970**, *2*, 215.
- (4) Van Den Bergh, H. E.; Callear, A. B. *Trans. Faraday Soc.* **1971**, *67*, 2017.
- (5) Pratt, G.; Veltman, I. *J. Chem. Soc., Faraday Trans. 1* **1976**, *72*, 2477.
- (6) Pilling, M. J.; Robertson, J. A.; Rogers, G. J. *Int. J. Chem. Kinet.* **1976**, *8*, 833.
- (7) Vakhtin, A. B.; Petrov, A. K. *Chem. Phys.* **1991**, *149*, 427.
- (8) Davies, J. W.; Green, N. J. B.; Pilling, M. J. *J. Chem. Soc., Faraday Trans.* **1991**, *87*, 2317.
- (9) Tucker, B. G.; Whittle, E. *Trans. Faraday Soc.* **1965**, *61*, 484.
- (10) Amphlett, J. C.; Macauley, L. J. *Can. J. Chem.* **1976**, *54*, 1234.
- (11) Masanet, J.; Caralp, F.; Ley, L.; Lesclaux, R. *Chem. Phys.* **1992**, *160*, 383.
- (12) McCoustra, M. R. S.; Pfab, J. P. *Spectrochim. Acta* **1990**, *46A*, 937.
- (13) Carmichael, P. J.; Gowenlock, G.; Johnston, C. A. F. *J. Chem. Soc., Perkin Trans. 2* **1973**, 1853.
- (14) Dyet, J. A.; McCoustra, M. R. S.; Pfab, P. J. *J. Chem. Soc., Faraday Trans.* **1988**, *84*, 463.
- (15) Glänzer, K. G.; Macir, M.; Troe, J. *Chem. Phys. Lett.* **1979**, *61*, 175.
- (16) Ellerman, T. Thesis, RISO National Laboratory, Roskilde, Denmark, 1991.
- (17) Rattigan, O. Thesis, National University of Ireland, Dublin, Ireland, 1991.
- (18) Lesclaux, R.; Caralp, F. *Int. J. Chem. Kinet.* **1984**, *16*, 117.
- (19) Caralp, F.; Lesclaux, R. *Chem. Phys. Lett.* **1983**, *102*, 54.
- (20) Danis, F.; Caralp, F.; Rayez, M. T.; Lesclaux, R. *J. Phys. Chem.* **1991**, *95*, 7300.
- (21) Lightfoot, P. D.; Veyret, B.; Lesclaux, R. *J. Phys. Chem.* **1990**, *94*, 700.
- (22) Clyne, M. A.; Walker, R. F. *J. Chem. Soc., Faraday Trans. 1* **1973**, *64*, 1547.
- (23) Danis, F.; Caralp, F.; Veyret, B.; Loirat, H.; Lesclaux, R. *Int. J. Chem. Kinet.* **1989**, *21*, 715.
- (24) Chemical Kinetics and Photochemical Data for use in Stratospheric Modeling. NASA-JPL Publication, 90-1, 1990.
- (25) Allston, T. D.; Fedyk, M. L.; Takas, G. S. *Chem. Phys. Lett.* **1978**, *60*, 97.
- (26) Timonen, R. S.; Russel, J. J.; Gutman, D. *Int. J. Chem. Kinet.* **1988**, *18*, 1193.
- (27) Roussel, P. B.; Lightfoot, P. D.; Caralp, F.; Catoire, V.; Lesclaux, R.; Forst, W. *J. Chem. Soc., Faraday Trans.* **1991**, *87*, 2362.
- (28) Ernsting, N. P.; Pfab, P. *J. Spectrochim. Acta* **1980**, *36A*, 75.
- (29) Dewar, M. J. S.; Thiel, W. *J. Am. Chem. Soc.* **1977**, *99*, 4899.
- (30) Dewar, M. J. S.; McKee, M. L.; Rzepa, H. S. *J. Am. Chem. Soc.* **1978**, *100*, 3607.
- (31) Hudgens, J. W.; Johnson, R. D.; Kafafi, S. *J. Am. Chem. Soc.* **1990**, *112*, 5763.
- (32) Hudgens, J. W.; Johnson, R. D.; Timonen, R. S.; Seetula, J. A.; Gutman, D. *J. Phys. Chem.* **1991**, *95*, 4400.
- (33) Lias, S. G.; Bartness, J. E.; Liebman, F.; Holmes, J. L.; Levin, R. D.; Mallard, W. G. *J. Phys. Chem. Ref. Data* **1988**, *17*, Supplement No. 1.
- (34) Forst, W. *QCPM* **1993**, *13*, 119.
- (35) Davies, J. W.; Pilling, M. J. Bimolecular Collisions. In *Advances in Gas Phase Photochemistry and Kinetics*; Ashfold, M. N. R., Baggott, J. E., Eds.; The Royal Society of Chemistry: Letchworth, Herts, 1989.
- (36) Gardiner, W. C.; Troe, J. In *Combustion Chemistry*; Gardiner, W. C., Ed.; Springer-Verlag: New York, 1984.
- (37) Wagner, A. F.; Wardlaw, D. M. *J. Phys. Chem.* **1988**, *92*, 2462.
- (38) Nielsen, O. J.; Ellerman, T.; Pagsberg, P.; Sidebottom, H. W.; Rattigan, O. To be submitted for publication.
- (39) Frisch, M. J.; Head-Gordon, M.; Schlegel, H. B.; Raghavachari, K.; Binkley, J. S.; Gonzalez, C.; Defrees, D. J.; Fox, D. J.; Whiteside, R. A.; Seeger, R.; Melius, C. F.; Baker, J.; Martin, R.; Kahn, L. R.; Stewart, J. J. P.; Fluder, E. M.; Topiol, S.; Pople, J. A. *GAUSSIAN 88*; Gaussian, Inc.: Pittsburgh, PA, 1988.
- (40) Hariharan, P. C.; Pople, J. A. *Chem. Phys. Lett.* **1972**, *66*, 217.
- (41) Defrees, D. J.; Raghavachari, K.; Schlegel, H. B.; Pople, J. A. *J. Am. Chem. Soc.* **1982**, *104*, 5576.
- (42) McMillen, D. F.; Golden, D. M. *Annu. Rev. Phys. Chem.* **1982**, *33*, 493.
- (43) Weissman, M.; Benson, S. W. *J. Phys. Chem.* **1983**, *87*, 243.
- (44) Russel, J. J.; Seetula, J. A.; Gutman, D.; Danis, F.; Caralp, F.; Lightfoot, P. D.; Lesclaux, R.; Melius, C. F.; Senkan, S. M. *J. Phys. Chem.* **1990**, *94*, 3277.
- (45) Forst, W. *J. Phys. Chem.* **1991**, *95*, 3612.
- (46) Forst, W.; Caralp, F. *J. Chem. Soc., Faraday Trans.* **1991**, *87*, 2307.
- (47) *JANAF Thermochemical Tables*; Stull, D. R., Prophet, H., Eds.; NSRDS-NBS 37, 2nd ed.; Government Printing Office: Washington, DC, 1971.